Demonstration of Unidirectional Single-Stranded DNA Translocation by PcrA Helicase: Measurement of Step Size and Translocation Speed†

Mark S. Dillingham,‡ Dale B. Wigley,*,‡ and Martin R. Webb§

Sir William Dunn School of Pathology, University of Oxford, South Parks Road, Oxford OX1 3RE, United Kingdom, and National Institute for Medical Research, Mill Hill, London NW7 1AA, United Kingdom

Received September 8, 1999; Revised Manuscript Received October 26, 1999

ABSTRACT: Using a fluorescent sensor for inorganic phosphate, the kinetics of ATP hydrolysis by PcrA helicase were measured in the presence of saturating concentrations of oligonucleotides of various lengths. There is a rapid phase of inorganic phosphate release that is equivalent to several turnovers of the ATPase, followed by slower steady-state ATP hydrolysis. The magnitude of the rapid phase is governed by the length of single-stranded DNA, while the slow phase is independent of its length. A kinetic model is presented in which the rapid phase is associated with translocation along single-stranded DNA, after the PcrA binds randomly along the DNA. There is a linear relationship between the length of single-stranded DNA and both the duration and amplitude of the rapid phase. These data suggest that the translocation activity occurs at 50 bases/s in unidirectional single-base steps, each requiring the hydrolysis of 1 ATP molecule.

DNA helicases are ubiquitous enzymes that couple the free energy of ATP hydrolysis to the separation of duplex DNA into its component single strands (for reviews see refs *1, 2*). Since this separation is a precursor to many types of DNA transactions, helicases are involved in virtually all aspects of DNA metabolism. DNA helicases have been classified into families according to primary structure (*3*) but can also be grouped on the basis of oligomeric state or polarity of DNA unwinding (*1, 2*). Although many helicases appear to function as either hexamers or dimers (*1*), some are monomeric, including the PcrA helicase used in this study (*4*−*6*). DNA helicases possess a strong polarity of DNA unwinding that relates to a unidirectional translocation of the enzyme with respect to the duplex being unwound. Most DNA helicases require a short piece of ssDNA[1] flanking the duplex for initiation of unwinding activity. This provides a convenient means to detect the translocation polarity of a helicase because the ssDNA can be attached to either the 3′ or 5′ side of the duplex (reviewed in ref *1*).

The nature and mechanism of DNA translocation by DNA helicases represent a fundamental area of their activity which remains poorly understood. ssDNA is a polar molecule, and an intuitive explanation for unwinding polarity is simply that the helicases track unidirectionally along the contour of a single DNA strand (Figure 1). Lee and Marians (*7*) have exploited the rare property of PriA as a site-specific helicase to demonstrate ssDNA translocation indirectly. By investigating the time taken to translocate between a PriA binding site and a target duplex region, they determined a net translocation speed of 90 bases/s. Matson and Richardson (*8*) have inferred that the T7 gene 4 protein translocates unidirectionally by examining the effect of ssDNA length on the concentration of ssDNA required to stimulate ATP hydrolysis half-maximally. Similar experiments have been performed with gp41 helicase to reach the same conclusion (*9*). Other groups have demonstrated the inhibitory effects on helicases of agents which prevent DNA tracking by providing a physical block along the DNA contour (*10*−*13*). Most recently, Morris and Raney (*14*) have demonstrated that the gp41 and Dda helicases are capable of displacing streptavidin from biotin-labeled DNA with a strong directional bias. This observation suggests that these helicases can generate significant directional force against a static blocking agent and is consistent with a unidirectional tracking event (Figure 1). However, a direct demonstration of unidirectional ssDNA tracking remains unavailable, and alternative explanations for unwinding polarity should be considered. One such hypothesis is that unwinding polarity

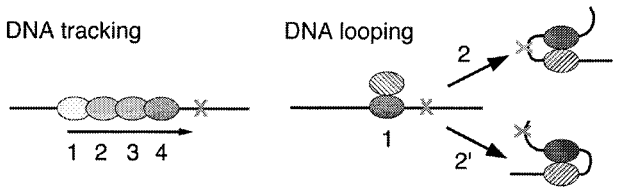

FIGURE 1: Possible mechanisms for ssDNA translocation in helicases. In a tracking model, the protein progresses unidirectionally along the contour of the DNA. It would either displace or be stopped by a static blocking agent as indicated by the cross. In a looping model, two subunits of the functional helicase progress without directional bias (as indicated by 2 and 2′). A static blocking agent (cross) can be "looped out" and bypassed.

† This work was supported by the Wellcome Trust (M.S.D., D.B.W.) and the Medical Research Council (M.R.W.).

* To whom correspondence should be addressed. Tel: +44 1865 285479. Fax: +44 1865 275515. E-mail: wigley@eric.path.ox.ac.uk.

‡ University of Oxford.

§ National Institute for Medical Research.

[1] Abbreviations: MDCC-PBP, phosphate binding protein modified at Cys197 with *N*-[2-(1-maleimidyl)ethyl]-7-(diethylamino)coumarin-3-carboxamide; ssDNA, single-stranded DNA; dsDNA, double-stranded DNA.

10.1021/bi992105o CCC: $19.00
Published on Web 12/09/1999

arises from the asymmetry imposed by structure of the ss/dsDNA interface (*1*). Indeed, it was recently proposed that the 3′-5′ polarity of the Sgs1 helicase of *Saccharomyces cerevisiae* is determined by binding specificity at the ss/dsDNA junction (*15*). Moreover, Amaratunga and Lohman (*16*) have demonstrated that *Escherichia coli* Rep is able to unwind helicase substrates into which "blocking" segments of poly(ethylene glycol) or reverse polarity DNA are added to the flanking ssDNA tail. A tracking movement along DNA should be unable to pass the DNA blocks. Therefore, these results have been interpreted as an indication that translocation takes place by the "looping out" of DNA between two subunits of a dimeric Rep enzyme (Figure 1). It was also suggested that Rep translocates ssDNA via looping interactions after examination of the equilibrium and kinetic constants for Rep dimerization and steady-state ATPase kinetics of cross-linked Rep·ssDNA complexes (*17*). The question of whether DNA helicases translocate by DNA looping or by unidirectional tracking along the contour of DNA remains unanswered.

The two translocation mechanisms of tracking and looping outlined above form the basis for helicase movement in two contrasting models for helicase activity. In the "active rolling model" of Wong and Lohman (*18*) progression of the helicase along the DNA is the result of DNA looping between the two subunits of a dimeric Rep helicase. Each subunit alternately binds ssDNA and dsDNA. This is controlled allosterically by negatively cooperative ATP binding and hydrolysis where Rep·ATP favors dsDNA binding, ATP hydrolysis melts dsDNA, and Rep·ADP favors ssDNA binding. This scheme produces a rolling motion in a C_2 symmetrical Rep dimer which results in translocation and dsDNA unwinding. The model predicts that translocation along ssDNA alone must occur in variable step sizes without directional bias and that it is the asymmetric structure of the ss/dsDNA junction that creates the polarity observed in the unwinding reaction. The step size for unwinding, associated with the binding and hydrolysis of 1 ATP molecule, must be at least as big as the binding site size of Rep plus the minimum amount of DNA required for the intervening loop. In the "inchworm" model originally described by Yarranton and Gefter (*19*) the helicase tracks along the contour of the DNA. A head site invades and melts duplex DNA, with the trailing tail site always bound to ssDNA. This model has been modified in the light of crystal structures of "substrate" and "product" complexes of PcrA helicase (*20*). In this modified "inchworm" model the helicase progresses along the contour of the DNA in steps of a single base which each requires the hydrolysis of 1 ATP molecule. The "inchworm" activity is a ssDNA tracking motor formed across the interdomain cleft of the enzyme. This is complemented by a structurally separate duplex destabilization activity that acts ahead of the progressing fork, initiating unwinding and presumably aiding ssDNA tracking.

We have studied the relationship between ATP hydrolysis and ssDNA translocation in *Bacillus stearothermophilus* PcrA helicase. Like the closely related *E. coli* Rep and UvrD proteins, PcrA is a 3′-5′ DNA helicase and a member of the helicase superfamily I (*3*). The DNA-dependent ATPase activity of PcrA has been characterized in the steady state (*4*). The rate of ATP hydrolysis catalyzed by PcrA is increased by 3 orders of magnitude in the presence of saturating quantities of ssDNA (*4, 21*). In the absence of accessory proteins, PcrA displays low processivity in vitro (*22*). Efficiency of unwinding rapidly drops for dsDNA >20 base pairs, and PcrA is unable to unwind an 81-base pair duplex (*22*). In this study we have examined the pre-steady-state kinetics of ATP hydrolysis by PcrA helicase in the presence of synthetic oligonucleotides of various lengths. Release of inorganic phosphate (P_i) from PcrA was monitored with a P_i sensor, a fluorescent coumarin-labeled phosphate binding protein (MDCC-PBP; *24*). The fluorescence emission of this sensor increases by ~8-fold on binding P_i, and this signal has been used to investigate the pre-steady-state kinetics of several ATPases (*23*−*25*). The protein binds P_i tightly ($K_D \sim 0.1\ \mu M$) and rapidly (rate constant $= 1.4 \times 10^8\ M^{-1}\ s^{-1}$ at 20 °C) (*23*). Under the conditions used in this work, essentially all P_i generated by ATP hydrolysis bind immediately to MDCC-PBP. Therefore the measured fluorescence change reflects the release of P_i from PcrA in both amplitude and kinetics. Stopped-flow techniques were used for these measurements and were performed under multiple turnover conditions; i.e., the concentrations of MDCC-PBP, ATP, and ssDNA were much greater than that of PcrA. In general, oligothymidylates of different lengths were used, because the steady-state ATPase activity of PcrA shows no selectivity for particular base sequences (*4*). Under these conditions, the P_i from each turnover of ATP hydrolysis can be observed before and after steady state is achieved and therefore gives a measure of ATPase activity in real time. The exception to this is for the first turnover, when P_i may be released at a rate faster than turnover if the rate-limiting step in the ATPase cycle follows P_i release (i.e. "burst kinetics").

The experiments show a rapid phase of P_i release whose amplitude is equivalent to multiple turnovers and is dependent upon the length of the ssDNA. This rapid phase is followed by a slower steady-state phase which is independent of the length of oligonucleotide. These data are interpreted in terms of a model in which the PcrA binds randomly to the DNA and rapidly moves to the 5′-end during the rapid phase of ATP hydrolysis. Using this model, the relationship between ssDNA length and ATP hydrolyzed enables quantification of the step size (bases per ATP) and translocation rate (bases per second).

EXPERIMENTAL PROCEDURES

Protein Preparation. MDCC-PBP (*23*, *25*) and PcrA helicase (*4*) were prepared as described. PcrA concentration was determined spectrophotometrically using a calculated extinction coefficient of 0.76 OD $mg^{-1}\ mL^{-1}\ cm^{-1}$ at 280 nm. In calculations of ATP turnover, it is assumed that all of the enzyme preparation is active.

Oligonucleotide Preparation. Oligonucleotides were synthesized using standard techniques (Val Cooper, Oxford University). They were then purified using ion-exchange chromatography on the ÄKTA purifier system (Pharmacia). After desalting with NAP-25 columns (Pharmacia), total DNA from either 0.2- or 1-μmol syntheses was loaded onto a 1-mL Resource Q column (Pharmacia) equilibrated in 10 mM NaOH, 250 mM NaCl. A linear salt gradient from 250 to 700 mM NaCl was then applied to the column to elute the DNA. This technique allows single-base resolution of

DNA for oligonucleotides of less than 20 bases. DNA was then exchanged into water using NAP-25 columns (Pharmacia) and concentrated at 60 °C in a vacuum concentrator (Eppendorf).

Stopped-Flow Measurements. Stopped-flow measurements were made with a Hi-Tech SF61MX apparatus, with excitation at 436 nm through 4-nm slits. Emission was measured after a 455-nm cutoff filter. All curves presented are single-trace measurements. All concentrations quoted are the final ones after mixing and were 0.1 μM PcrA, 500 μM ATP, and 3 μM MDCC-PBP unless otherwise stated. For investigation of the effect of ssDNA length and base composition on P_i release kinetics, the oligonucleotide concentration was 8 μM. All experiments were performed at 20 °C in a buffer containing 50 mM Tris·HCl (pH 7.5), 150 mM NaCl, and 3 mM $MgCl_2$. Due to the high affinity of MDCC-PBP for P_i and ubiquitous contamination by low levels of P_i, a P_i mop was used throughout to ensure that MDCC-PBP was P_i-free immediately prior to measurements. The P_i mop consists of 0.5 unit mL^{-1} bacterial purine nucleoside phosphorylase and 150 μM 7-methylguanosine (both from Sigma) which sequester P_i chemically as ribose-1-phosphate.

The fluorescence signal of MDCC-PBP was calibrated using known concentrations of P_i standard (Merck). Because of the very rapid binding of P_i to MDCC-PBP, it is not possible to obtain accurate amplitude information from this binding by mixing P_i and MDCC-PBP. So MDCC-PBP in solution conditions pertaining to the calibration was premixed with P_i (typically 0.1−1 μM) and then mixed in the stopped-flow apparatus with the enhanced P_i mop (*26*). This consists of 10 unit mL^{-1} purine nucleoside phosphorylase, 12.5 μg mL^{-1} phosphodeoxyribose mutase, 150 μM 7-methylguanosine, 25 μM $MnCl_2$, and 1 μM glucose-1,6-bisphosphate. The reduction in fluorescence was followed as the P_i dissociates from MDCC-PBP and is sequestered as ribose-5-phosphate.

Kinetic data were fitted to theoretical curves using either Hi-Tech IS-2 software or Grafit (version 3; Erithacus Software Ltd., Staines, U.K.). Kinetic simulations were performed using ModelMaker software (version 3; Cherwell Scientific Publishing, Oxford, U.K.).

RESULTS

The main aim of this work was investigation of the ATPase kinetics of PcrA in the presence of saturating concentrations of ssDNA of various lengths. To characterize these conditions fully and develop a kinetic mechanism, measurements were also done either in the absence of DNA or using sub-saturating concentrations. In addition, the kinetics were affected by the order of mixing PcrA, DNA, and ATP, and this was investigated using dT_{16}. Steady-state measurements under similar buffer conditions had shown that the K_m for ATP is 56 μM (*27*), and measurements here were mainly at 500 μM ATP, which was shown to be saturating with the dT_{16} oligonucleotide (data not shown).

P_i Release Kinetics for PcrA in the Absence of DNA. P_i release from PcrA immediately reached a steady-state rate of 0.13 s^{-1} without any burst phase (data not shown). This suggests that the rate-limiting step of DNA-independent ATP hydrolysis occurs at, or before, P_i release.

P_i Release Kinetics for PcrA with dT_{16}. The presence of ssDNA resulted in large changes in the kinetics of P_i release

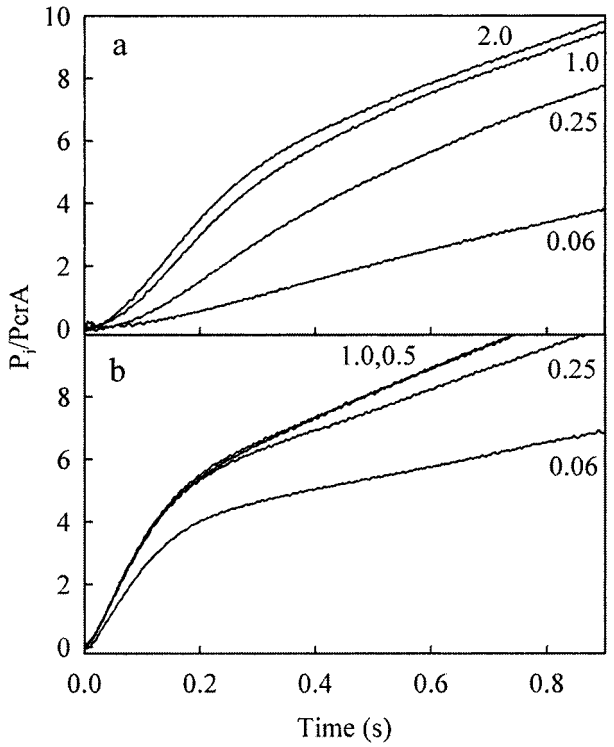

FIGURE 2: Kinetics of P_i release during PcrA interaction with dT_{16}. (a) 0.1 μM PcrA was mixed with 500 μM ATP and various concentrations of dT_{16} as indicated. (b) 0.1 μM PcrA was premixed with various concentrations of dT_{16} as indicated and then mixed with 500 μM ATP. The fluorescence signal was calibrated using known concentrations of P_i standard as described in the text.

(Figure 2a). When PcrA was mixed with saturating quantities of dT_{16} (>1 μM) and ATP, there was an initial lag phase, followed by a rapid multiturnover phase of P_i release, and finally a slower steady-state rate. A control experiment without PcrA showed no P_i release (data not shown). As [dT_{16}] was reduced, the phases merged, the lag increased, and the steady-state rate decreased. This will be interpreted below as being due to slow binding of PcrA to DNA directly corresponding to the lag and this slow binding controlling the steady-state rate at low [dT_{16}].

P_i Release Kinetics on Mixing PcrA·dT_{16} Complex with ATP. To investigate whether the lag phase was associated with DNA binding to PcrA, these measurements were repeated with preformed PcrA·dT_{16} complexes (Figure 2b). This preforming greatly reduces the lag phase while similar rapid and steady-state phases remain. Both main phases at saturating DNA concentrations are described quite well by simple linear equations, indicating two distinct and sequential processes, each governed by a different rate-limiting step. The rates of the rapid and steady-state phases are 40 and 6 s^{-1}, respectively, for the experiment shown in Figure 2b. To calculate the amplitude and duration of the rapid phase, we measured the total P_i release and the time, respectively, at the intercept of the two lines fitted to each phase of the reaction. This rapid phase amplitude corresponded to 5.6 ATP molecules hydrolyzed for each PcrA, and its duration was 170 ms. The traces at low [dT_{16}] show that the fast phase remains but becomes reduced in amplitude at sub-stoichiometric DNA concentrations, in agreement with the observation that DNA binds tightly to PcrA and the idea that the fast phase represents ATP hydrolysis during translocation,

Table 1: Relationship between Oligonucleotide Length and Rates of the Rapid and Steady-State Phases

oligonucleotide length (bases)	steady-state rate (s^{-1})	rate of rapid phase (s^{-1})
5	6.0	8.7
6	5.4	13.5
7	6.0	22.4
8	5.9	24.7
9	6.5	28.8
10	6.3	31.4
11	6.4	32.8
12	5.8	33.6
13	5.6	35.0
14	5.9	34.7
15	5.8	33.8
16	6.0	36
17	5.7	32

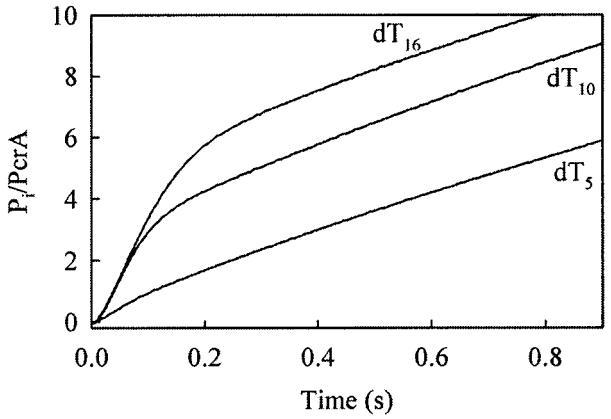

FIGURE 3: Kinetics of P_i release after premixing PcrA with poly(dT) of various lengths. 0.1 μM PcrA was premixed with 8 μM poly(dT) of various lengths (indicated) and then mixed with 500 μM ATP. Only the traces for three different ssDNA lengths are shown for clarity.

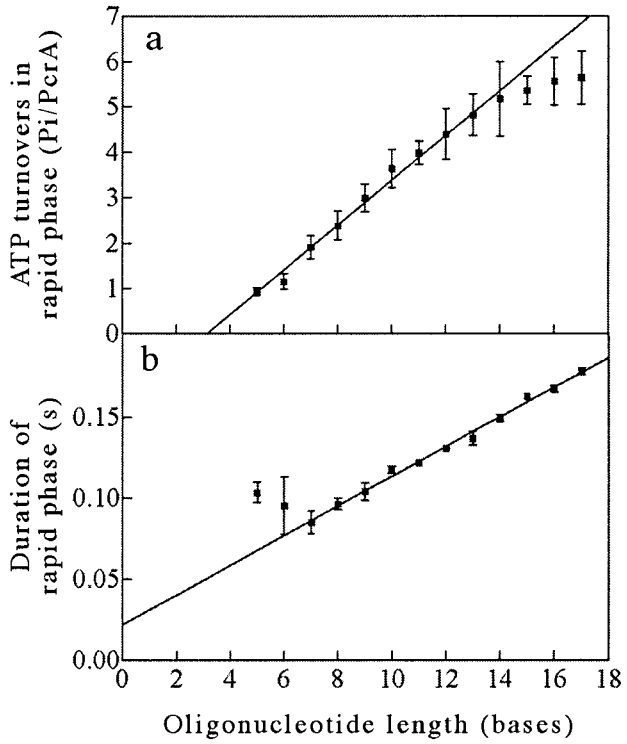

FIGURE 4: Relationship between oligonucleotide length, number of ATP molecules hydrolyzed per PcrA, and duration of the rapid phase. P_i released during the rapid phase is determined from the intercept of lines fitted to the two sequential phases of P_i release in the traces of Figure 3. ATP turnover (the P_i released per PcrA) (a) and duration of the rapid phase (b) are plotted as a standard deviation about a mean for independent experiments. The line fitted to the data in (a) excludes data from oligonucleotides over 14 bases in length (for reasons in the text) and has a slope of 0.49 ($\pm$0.02) P_i/base. The line fitted in (b) excludes data from oligonucleotides below 7 bases in length and has a slope of 109 ($\pm$2) bases/s.

i.e., before dissociation of PcrA·dT_{16}. The slow, steady-state phase does decrease in rate at very low [dT_{16}], and we will return to this point in the discussion of the kinetic mechanism of the ATPase cycle.

Effect of Oligonucleotide Length on the Rapid Phase. This was investigated using oligothymidylates from 5 to 17 bases in length (Table 1 and Figures 3 and 4). Saturating (8 μM) oligonucleotide was premixed with 0.1 μM PcrA. The concentration of oligonucleotide required to saturate PcrA was determined empirically for the shortest oligonucleotide investigated (dT_5) (data not shown). The saturating concentration for dT_5 (8 μM) was higher than that for dT_{16} (Figure 2), and so this concentration was used throughout. Under these conditions the vast majority of protein·DNA complexes contained a single PcrA monomer bound to a single oligonucleotide. The protein·DNA complex was then mixed with ATP as above.

The rate of the steady-state phase of the reaction is independent of the oligonucleotide used and is equal to ~6 s^{-1} in all cases (Table 1). This is consistent with the observation that the k_{cat} for steady-state ATP hydrolysis of PcrA is independent of the length of oligonucleotide (*4*). In contrast, the rate, amplitude, and duration of the rapid phase increase with length of oligonucleotide (Table 1 and Figure 4). Both the amplitude and the duration of the rapid phase show an approximately linear dependence on the length of oligonucleotide. Our interpretation of these data is that the rapid phases represent ATP hydrolysis coupled to ssDNA translocation. Each additional base results in an increase in the rapid phase amplitude equivalent to one-half an ATP for each PcrA molecule (Figure 4a). Also, the duration of the rapid phase increases by 9 ms for every additional base (Figure 4b). The deviations from linearity of the amplitudes with the longer oligonucleotides may be due to an increasing proportion of the DNA dissociating prematurely, i.e., before the 5′-end is reached. This is consistent with the observation that PcrA helicase is not very processive in vitro in the absence of additional protein components (*22*). The duration of the rapid phase also deviates from linearity, but at the lowest oligonucleotide lengths (Figure 4b).

Effect of DNA Sequence Composition on the Rapid Phase. Since the oligonucleotides in this study consist solely of thymine bases, we investigated how base composition affected the rapid phase of P_i release by PcrA·ssDNA complexes. The proposed model for ssDNA translocation in PcrA involves base flipping between sites of aromatic stacking interactions (*20*). Therefore, it is conceivable that the nature of the bases moving between the pockets could affect the macroscopic translocation rate, if the process is slow enough to contribute to rate limitation. To address this question experimentally we compared traces obtained with an 8-mer and a 10-mer of mixed base composition (5′-GTCACAGT and 5′-CGAGCACTGC) with those obtained for dT_8 and dT_{10}, respectively. The traces obtained for mixed

base oligonucleotides and polythymidylates of equivalent length were indistinguishable (data not shown).

DISCUSSION

In the absence of ssDNA, the slow basal ATPase activity of PcrA and lack of a P_i release burst are consistent with a minimal mechanism in which the hydrolysis step is rate limiting, as was found for the closely related Rep helicase of *E. coli* (*28, 29*). It is also expected from a mutational analysis of the nucleotide binding pocket of PcrA, which suggests that the stimulation of ATP hydrolysis afforded by ssDNA binding is linked to Mg^{2+} coordination and consequently to ATP hydrolysis (*21*). Addition of DNA causes an ~100-fold increase in steady-state ATPase activity. The rate of the second (steady-state) phase of this reaction is in reasonable agreement with a steady-state rate for DNA-dependent ATP hydrolysis of 11 s^{-1} measured using a coupled assay (*30*) under similar buffer conditions (data not shown). This phase is independent of ssDNA length (Table 1), but it is preceded by a rapid multiple turnover of ATP whose amplitude and duration are both linearly dependent upon ssDNA length.

The data for PcrA in the presence of ssDNA will be interpreted in terms of the model in Figure 5. Following PcrA association with DNA randomly along its length (step 1) and a conformation change, possibly induced by ATP binding (step 2), every ATP hydrolysis produces unidirectional movement by a single base toward the 5′-end (step 3) with tight coupling between ATP hydrolysis and movement along the DNA. During translocation, the rate-limiting step would either be associated with a component of ATP hydrolysis, the DNA translocation event, or the protein conformational changes associated with coupling these events. When the PcrA reaches the 5′-end of DNA, it hydrolyzes ATP more slowly without DNA movement (step 4) and the protein can also undergo slow dissociation (step 5). Once dissociated, the DNA and protein can reassociate (step 1) and the cycle begins again. The evidence will first be treated semiquantitatively to develop the model. The interpretation will then include a kinetic mechanism by estimating rate constants for each step. The extent to which the kinetic data and crystal structures (*20, 31*) are consistent with this model will also be discussed.

The comparison of data in Figures 2 and 3 provides strong evidence that the process of DNA binding is slow: a lag in the P_i release is almost entirely eliminated if the PcrA·DNA complex is preformed. However, as in Figure 2a, the lag is not eliminated at high [DNA] on mixing DNA with PcrA, and this suggests that there is two-step binding: binding itself followed by a conformation change. Evidence for a second kinetically significant step (step 2) between DNA binding and the start of ATP hydrolysis and translocation comes from the increase in rate of the rapid (translocation) phase with DNA length (Table 1). Without such a step, at least in measurements where PcrA·DNA is preformed, the rate of ATP hydrolysis during translocation would be independent of length. In that case, although the process would go on longer with more steps as the DNA length increases, each step would take the same time. If instead there is a slow step (step 2), with a rate that is independent of length, followed by rapid ATP hydrolysis with more ATPs hydrolyzed for the longer DNA, this produces the rate increase with DNA length that is observed and allows correlation of the stepping rate with that of the rapid phase. The existence of this slow step before translocation is also apparent in the relationship between rapid phase duration and oligonucleotide length (Figure 4b). These data do not extrapolate to zero time for a zero length oligonucleotide (discussed below). It is evident that the data for dT_5 and dT_6 do not fit to the trend displayed by all of the other oligonucleotides. In two crystal structures of PcrA bound to a partial duplex substrate, the protein contacts 5−6 bases of the ssDNA tail (20).

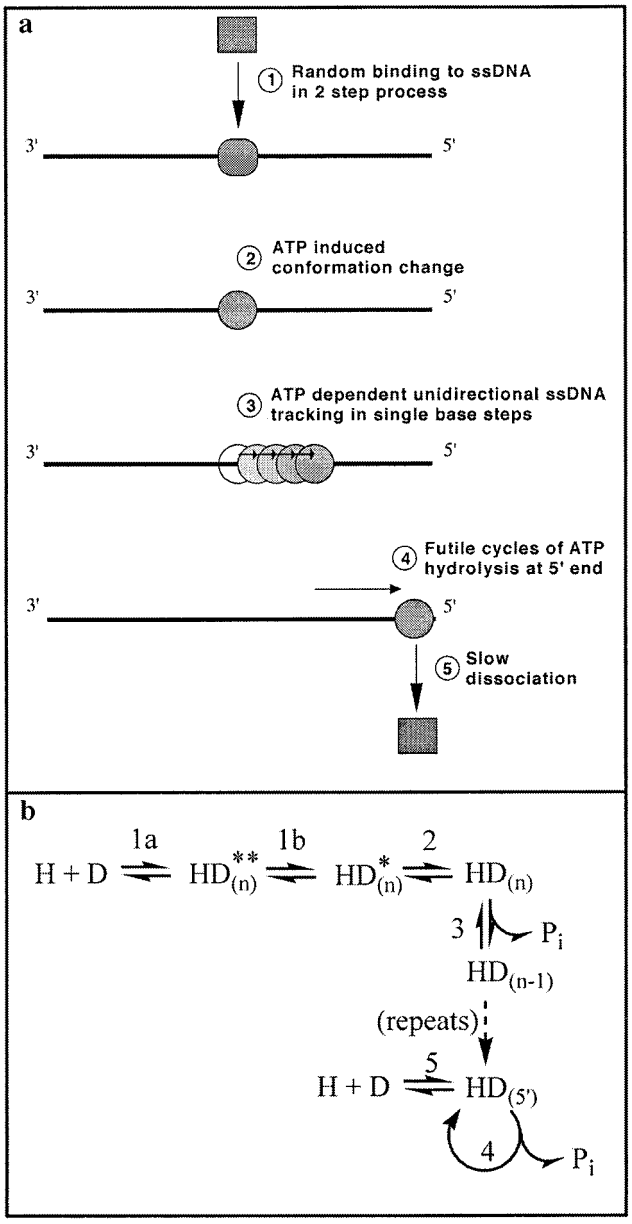

FIGURE 5: Mechanism of ssDNA translocation by PcrA helicase. (a) Cartoon model for ssDNA translocation by PcrA helicase: step 1, PcrA binds randomly along the length of ssDNA in a two-step process; step 2, a unique conformational change takes place on binding ATP which sets up the enzyme for translocation; step 3, PcrA tracks along DNA in a 3′-5′ direction, hydrolyzing 1 ATP for every base at a rate of 50 s^{-1}; step 4, ATP hydrolysis at the 5′-end at around 6 s^{-1}; step 5, rate-limiting dissociation and conformational change. (b) Kinetic scheme; see text for details. The asterisks represent different conformational states. H and D represent PcrA helicase and DNA, respectively, with the binding position along DNA shown in parentheses.

Therefore, one simple explanation for this anomaly is that the initial conformational change is slower with oligonucleotides that are shorter than the site size, and it may be that this event is related to a conformational change in the ssDNA binding site.

The data on the rapid phases with different lengths of ssDNA are interpreted as representing ATP hydrolysis coupled to translocation. Each additional base results in an increase in the rapid phase amplitude equivalent to one-half an ATP for each PcrA molecule (Figure 4a). Importantly, the linear nature of this relationship suggests that DNA translocation is strictly unidirectional. In a model where random binding is followed by a random walk (i.e. every individual step the helicase makes is equally likely to be toward the 5′- or 3′-end), the average number of steps required to reach the end of the DNA would be related to the square of its length (*32*). Although the data do not distinguish between a 3′-5′ or 5′-3′ translocation, the activity is presumably 3′-5′ because this is the directionality of PcrA detected in helicase assays (*4*). The linear dependence of amplitude on length suggests two possible extremes of binding model and step size, assuming tight coupling between movement and hydrolysis. First, PcrA could bind to the 3′-end of the ssDNA preferentially and translocate to the 5′-end in steps of 2 bases with each step requiring the hydrolysis of 1 ATP molecule. Alternatively, PcrA could bind randomly to ssDNA, so that the average distance traveled to the end of DNA is one-half of the oligonucleotide length. In this case, the translocation step is a single base, each requiring the hydrolysis of 1 ATP molecule. For a variety of reasons, the second model is more likely. First, the amplitude/length relationship obtained is linear at single-base resolution. If PcrA were to bind preferentially to DNA ends, then the molecules would be strongly synchronized at the start of translocation. This should produce a relationship in which we see distinct step increases in amplitude at every second base, especially with the short oligonucleotides used in this study. Second, PcrA binds effectively to circular M13mp18 ssDNA which does not possess ends (*4*).

A linear relationship is also observed between the duration of the rapid phase and the length of oligonucleotide (Figure 4b). Assuming initial random DNA binding (discussed above), the gradient of this line suggests a translocation rate of 50 bases/s. The line fitted to these data does not pass through the origin. In practice an extrapolation of the line to base length 3 may be more relevant, as this is where the rapid phase would have zero amplitude (intercept of the abscissa in Figure 4a). This suggests the existence of a single common event for translocation along all of the oligonucleotides which takes approximately 50 ms (i.e. a rate of $\sim$20 s^{-1}). We hypothesize that this is associated with an initial ATP-induced conformational change (step 2) before translocation begins as described above.

Eventually, the PcrA molecule reaches the 5′-end of DNA. Translocation probably ceases while the three final bases at the 5′-end of ssDNA are still bound to the enzyme. This is suggested by the fact that the P_i release amplitude (Figure 4a) extrapolates to zero at an oligonucleotide length of three bases. It is also consistent with crystal structures of PcrA helicase (20) which indicate that the rear section of the translocation machinery (domain 1A) binds three bases of ssDNA. ATP hydrolysis clearly continues at the 5′-end, and this is the slower steady-state phase. The steady-state rate is independent of DNA length and cannot, therefore, be described simply by a rate-limiting dissociation of the PcrA·DNA complex followed by recycling. In a "conventional" ATPase cycle, this slow dissociation would indeed lead to slower steady-state hydrolysis. However, in that case each complete cycle of DNA association, translocation, and dissociation generates a number of ATP turnovers which would be ssDNA length-dependent. This effectively means that the observed steady-state rate would be higher for longer oligonucleotides, and this is not observed. Instead, we explain the steady-state rate being independent of length by invoking the idea that the PcrA undergoes "futile cycles" of ATP hydrolysis at the 5′-end: ATP is slowly hydrolyzed but is uncoupled from DNA translocation. During this process, we envisage that the PcrA molecule might still undergo the ATP-dependent conformation changes that are required for translocation but be unable to progress further since a DNA end has already been reached. Now the steady-state rate is dominated by "futile cycling" at the 5′-end and is independent of length. In practice there must be dissociation, and it is assumed to occur occasionally but with insufficient frequency to affect the observed ATPase rate when DNA is saturating. The steady-state rate does become reduced at very low DNA concentrations (Figure 2), where dissociation and reassociation dominate. It should be noted that in vivo the protein will only very rarely experience a 5′-end.

With the above mechanism in mind, it is now possible to fit a set of kinetic constants to the observed data using the scheme in Figure 5a as a basis. The results of the modeling are represented in Figure 6. The kinetic scheme is that for the series of steps in Figure 5b, but assuming all are irreversible. (The lack of any burst kinetics means that there are no observations that require reversibility.) PcrA binds at random to all positions along the DNA, including the 5′-end, such that there are $n - 2$ binding sites where n is the number of bases. This models the amplitude of rapid phase P_i release correctly and is consistent with zero amplitude at a length of 3 bases (Figure 4a). The binding is in two steps, binding itself (step 1a) and a conformational change (step 1b) to account for the fact that the lag is not removed by mixing with increasing [DNA] (Figure 2a). Following binding there is a second conformational change (step 2), assumed to be ATP-induced and invoked to explain the rate dependence of the fast phase on changing lengths of DNA and to explain Figure 4b, as described above. Without such a step, the simulation fails to predict fully the decreased rate of rapid phase at short oligonucleotide lengths. Step 3 is translocation coupled to ATP hydrolysis and so is repeated until each PcrA molecule reaches the 5′-end. Thus the total P_i produced per PcrA during this fast phase is the average, $\{(n - 3) + (n - 4)...0\}/(n - 2)$. Once at the 5′-end the PcrA can hydrolyze ATP without translocation (step 4) or dissociate from DNA (step 5) and so begin another cycle. The rate constants used in the simulations are given in Figure 6. The simulations at three lengths of DNA (5, 10, and 16 bases) premixed with PcrA are shown in Figure 6a. It is the values of k_3, k_4, and k_5 that determine the main features, the slopes of the fast and slow phases. The simulation overestimates the size of the fast phase for longer DNA, as it does not take into account that the protein can dissociate before reaching the 5′-end. Figure 6b shows the effect of reducing

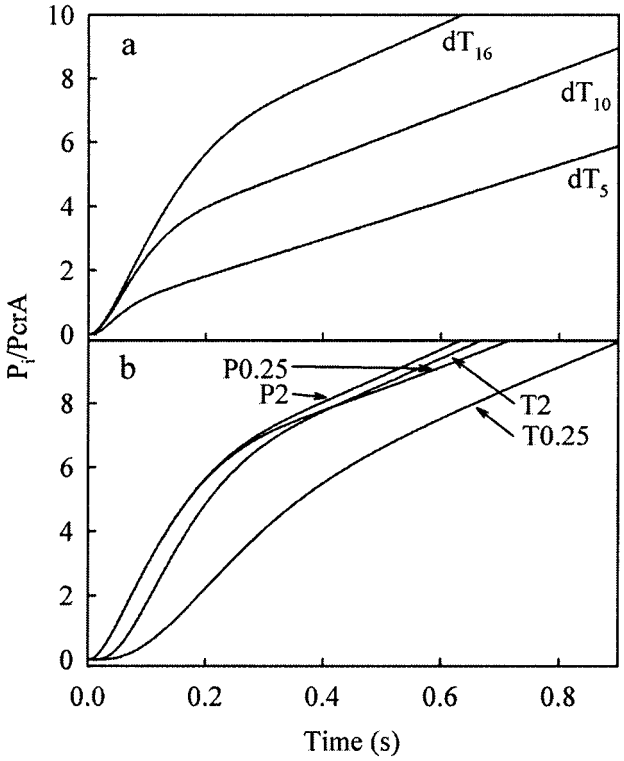

FIGURE 6: Simulation of P_i release kinetics using the mechanism in Figure 5. The forward rate constants are $k_{1a} = 3 \times 10^7$ M^{-1} s^{-1}, $k_{1b} = 60$ s^{-1}, $k_2 = 20$ s^{-1}, $k_3 = 50$ s^{-1}, $k_4 = 5.5$ s^{-1}, and $k_5 = 0.6$ s^{-1}. (a) PcrA (0.1 μM) is premixed with oligonucleotides of three lengths as indicated. (b) PcrA is premixed with a 16-mer (2 μM saturating and 0.25 μM labeled P2 and P0.25). The other traces show the effect of mixing the same DNA with PcrA at time zero (T2 and T0.25).

DNA concentration for a PcrA·dT_{16} complex and the increase in lag observed when DNA and PcrA are not premixed. In these traces, k_{1a} and k_{1b} are now important for determining the effect of DNA binding. Further refinement of the kinetic model will require individual rate constants (such as those for PcrA·DNA association and dissociation) to be tested by other methods. Even so, the simulations are good fits to the experimental data and provide confidence in the proposed mechanism.

The results presented above provide a demonstration of the DNA translocation component of helicase activity. Moreover, these data allow us to make quantitative estimates of the coupling ratio of ATP hydrolysis and ssDNA translocation. Assuming random DNA binding at the outset, and that all ATP turnovers are productive, the data show that 1 ATP is required for every base of translocation. These data cannot discount the possibility that PcrA actually progresses in larger increments: it is formally possible that free energy from multiple ATP turnovers could somehow be stored in the enzyme and finally released in a fast step to produce a movement of an equal number of bases. However, the fact that the relationship between ATP turnover and distance translocated is linear at single-base resolution (rather than having a steplike relationship) and consideration of the available structures of PcrA (*20*, *31*) points to the simpler model that the step size is actually 1 base. Although this step size has been measured for ssDNA translocation only, it seems likely that the same mechanism will be employed as the enzyme moves through duplex DNA during full helicase activity. A "coupling ratio" of 1 ATP/base is thermodynamically rather inefficient, as it has been estimated that the free energy associated with the hydrolysis of 1 ATP molecule could separate anywhere between 2 and 4 base pairs (*33*) and 9−12 base pairs (*1*). This corresponds to a restraint for a minimum possible coupling ratio of about 0.1 ATP/base. However, a higher coupling ratio may be required to translocate through particularly stable DNA duplexes, such as those which are bound to other proteins or display particular topologies. Several groups have measured the macroscopic efficiency of helicase activity in the *E. coli* helicases Rep and RecBCD, and their estimates vary between 1 and 3 ATP molecules/base pair (*19*, *33*−*36*, reviewed in ref *1*). The measurements were made by indirect methods, and it had been suggested previously that the apparently poor thermodynamic efficiency was related to substantial uncoupled ATP hydrolysis in these systems in vitro (*1*). Given that the step size of ssDNA translocation in PcrA helicase is 1 ATP/base, the observed thermodynamic inefficiency of these helicases during DNA unwinding might now be explained by the tracking mechanism itself, with uncoupled ATP hydrolysis playing a less significant role.

The small step size for ssDNA translocation and the linear relationship between rapid phase amplitude and oligonucleotide length are inconsistent with a DNA looping mode of ssDNA translocation and consequently with the "active rolling model" (*18*) for helicase activity. Instead these data point to the unidirectional ssDNA tracking mode for ssDNA translocation that is a feature of the "inchworm" model (*19*, *20*). Importantly, they are also consistent with crystal structures of "substrate" and "product" complexes of PcrA helicase (*20*). Upon the basis of the differences between these two complexes, a detailed structural mechanism has been proposed for PcrA-catalyzed helicase activity in which the protein progresses by tracking along ssDNA with a step size of 1 base for each ATP hydrolyzed (*20*). The data presented here provide the first experimental measurement, for any helicase, of the stoichiometry of the coupling of ATP hydrolysis to unidirectional stepwise movement. The data also provide a translocation speed of 50 s^{-1}, albeit with ssDNA. However, this does provide a basis for investigating DNA structural phenomena which might alter ssDNA translocation speed, not least the presence of duplex DNA ahead of the progressing ssDNA motor.

ACKNOWLEDGMENT

We thank Dr. Panos Soultanas and Dr. Alex Belton for useful discussions, Val Cooper for the synthesis of oligonucleotides, and Jennifer Byrne for technical assistance.

REFERENCES

1. Lohman, T. M., and Bjornson, K. P. (1996) *Annu. Rev. Biochem. 65*, 169−214.
2. Bird, L. E., Subramanya, H. S., and Wigley, D. B. (1998a) *Curr. Opin. Struct. Biol. 8*, 14−18.
3. Gorbalenya, A. E., and Koonin, E. V. (1993) *Curr. Opin. Struct. Biol. 3*, 419−429.
4. Bird, L. E., Brannigan, J. A., Subramanya, H. S., and Wigley, D. B. (1998b) *Nucleic Acids Res. 26*, 2686−2693.
5. Mechanic, L. E., Hall, M. C., and Matson, S. W. (1999) *J. Biol. Chem. 274*, 12488−12498.

6. Porter, D. J. T., Short, S. A., Hanlon, M. H., Preugschat, F., Wilson, J. E., Willard, D. H., and Consler, T. G. (1998) *J. Biol. Chem. 273*, 18906−18914.
7. Lee, M. S., and Marians, K. J. (1990) *J. Biol. Chem. 265*, 17078−17083.
8. Matson, S. W., and Richardson, C. C. (1983) *J. Biol. Chem. 258*, 14009−14016.
9. Young, M. C., Schultz, D. E., Ring, D., and von Hippel, P. H. (1994) *J. Mol. Biol. 235*, 1447−1458.
10. Brown, W. C., and Romano, L. J. (1989) *J. Biol. Chem. 264*, 6748−6754.
11. Maine, I. P., and Kodadek, T. (1994) *Biochem. Biophys. Res. Commun. 198*, 1070−1077.
12. Naegeli, H., Bardwell, L., and Friedberg, E. C. (1992) *J. Biol. Chem. 267*, 392−398.
13. Raney, K. D., and Benkovic, S. J. (1995) *J. Biol. Chem. 270*, 22236−22242.
14. Morris, P. D., and Raney, K. D. (1999) *Biochemistry 38*, 5164−5171.
15. Bennett, R. J., Keck, J. L., and Wang, J. C. (1999) *J. Mol. Biol. 289*, 235−248.
16. Amaratunga, M., and Lohman, T. M. (1993) *Biochemistry 32*, 6815−6820.
17. Wong, I., and Lohman, T. M. (1996) *Proc. Natl. Acad. Sci. U.S.A. 93*, 10051−10056.
18. Wong, I., and Lohman, T. M. (1992) *Science 256*, 350−355.
19. Yarranton, G. T., and Gefter, M. L. (1979) *Proc. Natl. Acad. Sci. U.S.A. 76*, 1658−1662.
20. Velankar, S., Soultanas, P., Dillingham, M. S., Subramanya, H. S., and Wigley, D. B. (1999) *Cell 97*, 75−84.
21. Soultanas, P., Dillingham, M. S., Velankar, S. S., and Wigley, D. B. (1999) *J. Mol. Biol. 290*, 137−148.
22. Soultanas, P., Dillingham, M. S., and Wigley, D. B. (1999) *Nucleic Acids Res. 26*, 2374−2379.
23. Brune, M., Hunter, J. L., Corrie, J. E. T., and Webb, M. R. (1994) *Biochemistry 33*, 8262−8271.
24. White, H. D., Belknap, B., and Webb, M. R. (1997) *Biochemistry 36*, 11828−11836.
25. Brune, M., Hunter, J. L., Howell, S. A., Martin, S. R., Hazlett, T. L., Corrie, J. E. T., and Webb, M. R. (1998) *Biochemistry 37*, 10370−10380.
26. Nixon, A. E., Hunter, J. L., Bonifacio, G., Eccleston, J. F., and Webb, M. R. (1998) *Anal. Biochem. 265*, 299−307.
27. Dillingham, M. S., Soultanas, P., and Wigley, D. B. (1999) *Nucleic Acids Res. 27*, 3310−3317.
28. Moore, K. J. M., and Lohman, T. M. (1994a) *Biochemistry 33*, 14550−14564.
29. Moore, K. J. M., and Lohman, T. M. (1994b) *Biochemistry 33*, 14565−14578.
30. Pullman, M. E., Penefsky, H. S., Datta, A., and Racker, E. (1960) *J. Biol. Chem. 235*, 3322−3329.
31. Subramanya, H. S., Bird, L. E., Brannigan, J. A., and Wigley, D. B. (1996) *Nature 384*, 379−383.
32. Grimmet, G. R., and Stirzaker, D. R. *Probability and Random Processes* (2nd ed.) pp 73−74, Oxford University Press, Oxford, U.K.
33. Roman, L. J., and Kowalczykowski, S. C. (1989) *Biochemistry 28*, 2873−2881.
34. Kornberg, A., Scott, J. F., and Bertsch, L. L. (1978) *J. Biol. Chem. 253*, 3298−3304.
35. Arai, N., and Kornberg, A. (1981) *J. Biol. Chem. 256*, 5294−5298.
36. Korangy, F., and Julin, D. A. (1994) *Biochemistry 33*, 9552−9560.

BI992105O